# I.T.C

# Sensorless Control of PMSM using Sliding Mode Observer in Solar Electric Tuktuk Application

Piseth Thok[1*], Bunthern Kim[2], Sokchea Am[2]

[1] Mechatronic, Information, Communication Engineering, Institute of Technology of Cambodia, Russian Federation Blvd., P.O. Box 86, Phnom Penh, Cambodia
[2] Department of Electrical and Energy Engineering, Institute of Technology of Cambodia, Russian Federation Blvd., P.O. Box 86, Phnom Penh, Cambodia

**Abstract:** *This article presents a sensorless control system of permanent magnet synchronous motor (PMSM) for solar electric tuktuk (E-tuktuk) application. This study purposes a new method of control algorithm of PMSM for E-tuktuk with low-cost by using the sensorless strategy. The sensorless strategy covers the estimated rotor speed and position of PMSM, and a sliding mode observer (SMO) is proposed in this study. The SMO is the most popular method of sensorless control because of its nonlinear control structure, deterministic nature, robustness, and high performance. The sigmoid function is used to reduce the chattering in the observer system. The Field Oriented Control (FOC) is a popular control algorithm because it is based on two fundamental ideas; flux and produced torque that can be controlled separately. The FOC was originally developed for medium-high performance motor applications that were required to operate smoothly over the full speed range and had an excellent dynamic performance. The proposed control algorithm is simulated by using MATLAB/Simulink, and the performance of the system is analyzed and developed. The simulation results indicate that the proposed method in this case study is capable of tracking the actual values of rotor speed and position of PMSM with small deviations, robustness, high dynamic performance, and sufficient for precise control. Lastly, this study is considered the first stepping stone toward real experiments with real parameters to confirm the performance in future work.*

## 1. INTRODUCTION

Permanent magnet synchronous motor (PMSM) is a widely used electric motor for an electric vehicle or hybrid electric vehicle (EV/HEV) application because of its simple structure, small size, lightweight, small inertia, high power density, with very suitable for limited space as EVs. Furthermore, its high efficiency, high power factor, torque to inertia, robustness, and high output torque, particularly at low speeds, make it ideal for starting and acceleration [1].

Currently, there are many control strategies and algorithms for PMSM. The vector control is characterized by high accuracy, sensitivity, wide speed range, and a simple control system. The control techniques method was proposed in the literature for the motor drive control. Fuzzy logic control (FLC) usually provides a nonlinear controller that was capable of performance that is different complex nonlinear control actions even for uncertain

nonlinear systems [2]. The voltage/frequency (V/F) control technique is the method that controls the output torque under constant air gap flux and does not require rotor position, as described in Semenov et al. [1], W. J. Kim and Kim, [3]. Direct torque control (DTC) controls the magnitude and the angle of the flux vector concerning the flux of the permanent magnets to achieve the desired output [4-6]. Field Oriented Control (FOC), the vector control of this algorithm was based on two fundamental ideas; flux and torque producing which can be controlled separately. FOC was originally developed for medium-high performance motor applications that were required to operate smoothly over the full speed range and had excellent dynamic performance [7,8].

The conventional position sensor not only adds the motor volume and shaft rotation inertia but also reduces the powder density of the motor. The position sensor increases the complexity of the motor structure, as well as the price and

difficulty of maintenance [9]. The sensorless control system can determine the rotor position in real-time by measuring the current and voltage of the port motor. Sensorless speed and position estimation are the widely desired need for high-performance permanent magnet motor drives to save costs, shrink size, and increase dependability. Many researchers have studied sensorless control strategies for multi-phase PMSMs, such as Kalman filter (KMF) and Extended Kalman filter (EKF) has been widely studied [10-13]. It can effectively suppress the influence of system error and measurement error on state estimation and improve accuracy. Luenberger observer was used for developing robustness estimation concerning measurement noise. Luenberger utilized some measurable states in the estimation results. The pole assignment of the system was optimized to get better dynamic performance [14,15]. Model reference adaptive system (MRAS) is an easy way to achieve sensorless control and the major advantage brought by the strategy is simple to design, robust to disturbance, insensitive to machine parameters, and high dynamic performance [11,15,16]. Back electromagnetic force (Back-EMF) observer was presented in Yousfi et al., [17], Urbanski, [10], Bedetti et al., [18], Lee, [19]. Extended state observer (ESO) was introduced as the second observer in cascade structure to improve the rotor speed estimation accuracy and fast response [20,21]. Maximum torque per ampere (MTPA) operation with two control loops based on the d-axis current. This technique requires a complex control algorithm with two PI controllers, and two arctangent functions were utilized in the stabilization process [3]. Sliding mode observer (SMO) is the most popular method because of its nonlinear control structure, deterministic nature, robustness, and high-performance [11,22]. The problem of chattering caused by the discontinuous switching function causes system oscillation and instabilities [23], which has been addressed by using higher-order SMO and filtering methods. The implementation of the sigmoid-based SMO, and hybrid SMO was computationally intensive [24]. The advantages of sigmoid function over signum function are presented in [25,26]. To avoid the low pass filter (LPF), replacing the signum function with a hyperbolic tangent function, and solving the problem of calculation delay with a current pre-compensation approach based on dual sampling technique in one sample interval [24,27].

In cities, auto-rickshaws or tuktuk are the common public transportation mode of last-mile connectivity. In this case, the author wants to modify the ICEs of the fuel tuktuk to the electric tuktuk (E-tuktuk) instead. The basic structure of any E-tuktuk involves an energy storage system (ESS) including the batteries, ultra-capacitors, etc., and an electric propulsion system (EPS) which includes an electric motor and a power electric converter as shown in Fig. 1.

This study presented the sensorless control of PMSM using sliding mode observer for the solar E-tuktuk application. The proposed sensorless sliding mode replaces the traditional sliding mode signum function with the sigmoid function. To define the state estimation problem for PMSM, the system and measurement have been modeled. The study of this topic is crucial for developing an accurate PMSM mathematical model and deciding which algorithm to use to estimate the speed and position of the motor rotor in the next step. The authors propose an estimation scheme to weaken chattering. The Sliding mode observer and PI controller are to determine the difference between the estimated position and the actual rotor position to zero. Natural chattering is eliminated, and the robustness of the rotor position and rotor speed estimation is improved. Starting from this control algorithm, the simulation study is proposed. MATLAB/Simulink is used to design and simulate the results of the system.
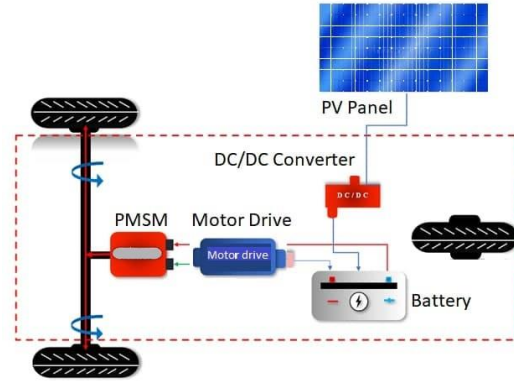


**Fig. 1.** Solar E-tuktuk System

## 2. SYSTEM MODELING

### 2.1 PMSM model

In general, the dynamic model of a PMSM with the rotor reference frame can be described as:

$$v_s = Ri_s + L\frac{di_s}{dt} + e_s \qquad \text{(Eq. 1)}$$

where $v_s$ are the voltage vector of phases *a, b, c*
$i_s$ are the current vector of phases *a, b, c*
$e_s$ are the induced electromotive force of phases *a, b, c*
$R$ is the winding resistance of phases *a, b, c*
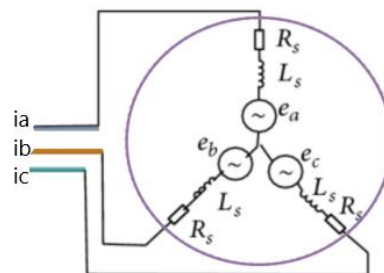$L$ is the winding inductance of phases *a, b, c*



**Fig. 2.** Electrical Schematic of a PMSM

The mechanical of PMSM presented as torque production is given as below:

$$T_{em} = J_m \frac{d\omega}{dt} + B\omega + T_L \qquad \text{(Eq. 2)}$$

where $T_{em}$ is the mechanical torque

$J_m$ is the moment of inertia

$B$ is the viscous friction

$\omega$ is the rotor angular velocity

$T_L$ is the load torque

After simplification, the mathematical model of PMSM in the stationary frame ($\alpha\beta$ frame) can be expressed:

$$\begin{cases} v_\alpha = Ri_\alpha + L\dfrac{di_\alpha}{dt} + e_\alpha \\[2mm] v_\beta = Ri_\beta + L\dfrac{di_\beta}{dt} + e_\beta \end{cases} \qquad \text{(Eq. 3)}$$

where:

$$e_\alpha = -\lambda\omega\sin\theta_e$$
$$e_\beta = \lambda\omega\sin\theta_e$$

and $\omega, \theta_e, \lambda, v_\alpha, v_\beta, i_\alpha, i_\beta, R, L$ are electric angular speed, rotor electric angle, rotor magnetic flux, $\alpha$-axis voltage, $\beta$-axis voltage, $\alpha$-axis current and $\beta$-axis current, rotor resistance, and inductance winding respectively.

The value of the produced electromagnetic torque in the $\alpha\beta$ reference frame can be described using the following expression:

$$T_e = \frac{3}{2}P(\lambda_\alpha i_\beta - \lambda_\beta i_\alpha) \qquad \text{(Eq. 4)}$$

where $T_e$, $P$, $\lambda_\alpha$, $\lambda_\beta$ are produced torque, poles pare, $\alpha$-axis and $\beta$-axis flux respectively.

*2.2 Sliding mode observer*

The sliding mode observer for estimating rotor position is based on the stator current estimator using discontinuous control. Only stator currents are directly measurable in the PMSM drive. The sliding mode surface is defined as:

$$S(x) = 0$$
$$S = i_s - i_s$$

Directly measurable in a PMSM drive, the sliding mode manifold is $S(x) = 0$.

Sliding mode observers of PMSM are defined as:

$$\begin{cases} \dfrac{d\hat{i}_\alpha}{dt} = -\dfrac{R}{L}\hat{i}_\alpha + \dfrac{1}{L}v_\alpha - K(sign(\bar{i}_\alpha)) \\[2mm] \dfrac{d\hat{i}_\beta}{dt} = -\dfrac{R}{L}\hat{i}_\beta + \dfrac{1}{L}v_\beta - K(sign(\bar{i}_\beta)) \end{cases} \qquad \text{(Eq. 5)}$$

where $\bar{i}_\alpha = \hat{i}_\alpha - i_\alpha$, $\bar{i}_\beta = \hat{i}_\beta - i_\beta$, $\hat{i}_\alpha$ and $\hat{i}_\beta$ represents the current error of $\alpha$-axis, the current error of $\beta$-axis, the current estimation of $\alpha$-axis, and the current estimation of $\beta$-axis respectively.

$sign(x)$ is the signum function of the traditional control equation of SMO, which has a serious chattering problem presented in [23] . To suppress the chattering phenomenon, replacing the signum function with the continuous sigmoid function was used in [24] , which is defined as:

$$sigmoid(x) = \frac{2}{1 + \exp(-\alpha x)} - 1 \qquad \text{(Eq. 6)}$$

where $\alpha$ is a positive constant and its value affects the convergence property of the function (used to adjust the sharpness of the transition between lower and upper bounds). Then SMO of PMSM can be expressed as:

$$\begin{cases} \dfrac{d\hat{i}_\alpha}{dt} = -\dfrac{R}{L}\hat{i}_\alpha + \dfrac{1}{L}v_\alpha - K(sigmoid(\bar{i}_\alpha)) \\[2mm] \dfrac{d\hat{i}_\beta}{dt} = -\dfrac{R}{L}\hat{i}_\beta + \dfrac{1}{L}v_\beta - K(sigmoid(\bar{i}_\beta)) \end{cases} \qquad \text{(Eq. 7)}$$

where $K$ is the switching gain of the discontinuous control and normal positive.

*2.3 Stability analysis*

Lyapunov function:

$$V = \frac{1}{2}S^T S \qquad \text{(Eq. 8)}$$

$$V = \frac{1}{2}\begin{bmatrix} \bar{i}_\alpha & \bar{i}_\beta \end{bmatrix}^T \cdot \begin{bmatrix} \bar{i}_\alpha & \bar{i}_\beta \end{bmatrix} = \frac{1}{2}\begin{bmatrix} \bar{i}_\alpha^2 + \bar{i}_\beta^2 \end{bmatrix} > 0 \qquad \text{(Eq. 9)}$$

From the Lyapunov stability theorem, the sliding mode condition can be derived to satisfy condition $V > 0$ and $\dot{V} < 0$ where $\dot{V} = S^T \dot{S}$

The error equation can be determined by (Eq. 7) and (Eq. 3) as equation (Eq. 10):

$$\begin{cases} \dfrac{d\bar{i}_\alpha}{dt} = -\dfrac{R}{L}\bar{i}_\alpha + \dfrac{1}{L}e_\alpha - K(sigmoid(\bar{i}_\alpha)) \\[2mm] \dfrac{d\bar{i}_\beta}{dt} = -\dfrac{R}{L}\bar{i}_\beta + \dfrac{1}{L}e_\beta - K(sigmoid(\bar{i}_\beta)) \end{cases} \qquad \text{(Eq. 10)}$$

From the (Eq. 8) and (Eq. 10), the time derivative of Lyapunov function can be written as:

$$\dot{V} = S^T\dot{S} = \bar{i}_\alpha\dot{\bar{i}}_\alpha + \bar{i}_\beta\dot{\bar{i}}_\beta \qquad \text{(Eq. 11)}$$

$$\dot{V} = \frac{1}{L}(\bar{i}_\alpha e_\alpha - K\bar{i}_\alpha(sigmoid(\bar{i}_\alpha)))$$
$$+ \frac{1}{L}(\bar{i}_\beta e_\beta - K\bar{i}_\beta(sigmoid(\bar{i}_\beta)))$$
$$- \frac{R}{L}(\bar{i}_\alpha^2 + \bar{i}_\beta^2) < 0$$

where the observer gain *K* can be derived to satisfy $\dot{V} < 0$ as:

$$K \geq \max(|\hat{e}_\alpha|, |\hat{e}_\beta|) \qquad \text{(Eq. 12)}$$

where $\hat{e}_\alpha, \hat{e}_\beta$ represented the back EMF estimations in α, β frames respectively.

The chattering problem is solved and the estimation is proved to be stable.

From back-EMF voltages, estimated rotor speed and position can be expressed as [24].

$$\hat{\omega}_r = \frac{\sqrt{\hat{e}_\alpha^2 + \hat{e}_\beta^2}}{\lambda} \qquad \text{(Eq. 13)}$$

$$\hat{\theta} = -\arctan\frac{\hat{e}_\alpha}{\hat{e}_\beta} \qquad \text{(Eq. 14)}$$

where $\hat{e}_x = K(sigmoid(x)) = K\frac{2}{1+\exp(-ax)} - 1$

## 3. SIMULATION STUDY

After finishing the system modeling in part 2, the simulation study is discussed in this section. Starting with speed control, FOC was applied to the control method of PMSM. The block diagram of vector control is shown in Fig. 3. There are three feedback loops, two are current loops and one is speed loop. Three-phase stator current *abc* are measured from the sensor then convert to *dq* reference frame using Park's transformation for current loops and converted to *αβ* reference frame using Clark's transformation for speed loop. The outer loop is the speed loop where speed is estimated by an SMO observer and compared with the reference value. The speed PI controller is controlling the error generating reference value for quadrature axis current $i_q$. The error between reference value $i_q$ and measured value $i_q$ is given to the PI controller generating $v_q$. The reference value of the direct axis current $i_d$ is zero for maximum torque. The PI controller works on this error generating $v_d$. The output of these two PI current controllers generates reference signals for the current controller to generate the switching signals for the inverter used in PMSM.

The simulation testing is done in MATLAB/Simulink. The SMO observer block is designed following equations (Eq. 13) and (Eq. 14) for estimating the rotor speed and position of PMSM. Fig. 4 shows the SMO system block diagram. The system's results were compared to the values measured in the control system's output. The block diagram parameters have been adjusted according to the experimental components and
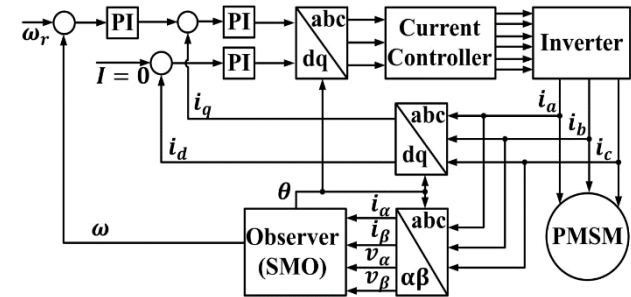
the values of the calculations.
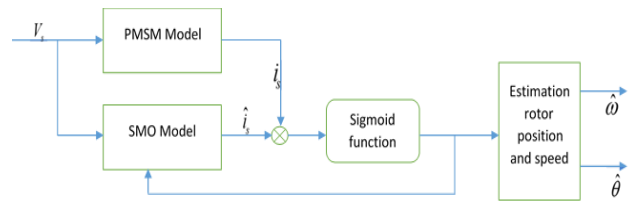


**Fig. 3.** Sensorless Control of PMSM



**Fig. 4.** Sliding Mode Observer Block

The parameters of the PMSM motor used in this study are given in Table 1.

**Table 1** Parameters of PMSM

| Parameters | Value | Unit |
|---|---|---|
| Rated power | 1 | KW |
| Rated voltage | 220 | V |
| Rated current | 4.4 | A |
| Rated speed | 262 | Rad/s |
| Rated torque | 4 | N.m |
| Rotor inertia | $2.97\times10^{-4}$ | Kg.m$^2$ |
| Resistance | 1.83 | Ω |
| Inductance | 4.72 | mH |
| Flux linkage | 0.175 | Wb |
| Frictional Constant | 0.0001 | N.m.s |
| Pole pairs | 4 | |

## 4. RESULTS SIMULATION

The simulation is carried out by showing the speed of PMSM for 4 different conditions. In case 1, the motor is running with speed change without load. In case 2, the motor is running with the speed change and with load torque at 4 N.m. In case 3, the motor is running at a constant speed with the load varies and in case 4, the motor is running at speed change with varying load.
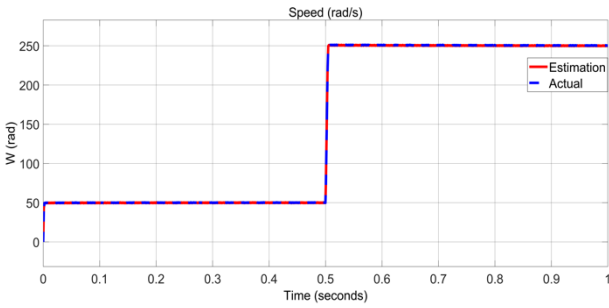
**Fig. 5.** Actual and estimated speed of PMSM with no load

In case 1, the response performance and robustness of the system (SMO Observer) with varying speeds of the motor from 50 *rad/s* to 250 *rad/s* at 0.5 *second* without load are verified. The simulation results are shown in Fig. 5, It can be seen that the estimated rotor speed is consistent with the actual rotor speed. When the motor started, the speed of the motor started from 0 to 50 *rad/s* immediately then the motor increased its speed to 250 *rad/s* immediately at 0.5 *second*. The estimated speed can quickly follow the set speed and converge to the actual speed, which shows that the system has good dynamic and static performance.
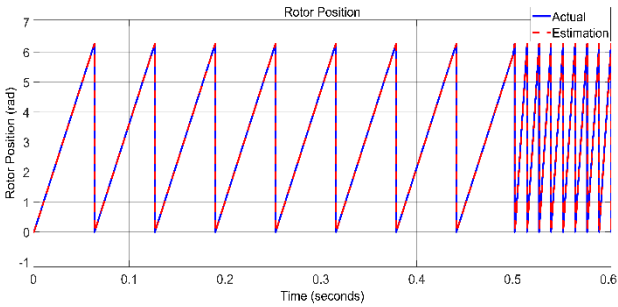


**Fig. 6.** Actual and estimated position of PMSM with no load

Fig. 6 shows the comparisons of actual and estimated values of rotor position while running at varying speeds and no-load. It can be seen that the estimated rotor position can maintain good consistency with the actual rotor position, which shows that the observer (SMO) has a good estimation effect. The controller (SMO) is well tracking with the actual position of PMSM whatever the speed is changed at 0.5 *seconds*. The rotor position will change the wavelength when the speed of PMSM is varied. The estimated angle is the same as the actual angle, which effectively weakens the high-frequency noise and harmonics in the back EMF and makes the output stable, and the control effect meets the performance control requirements of PMSM.

Fig 7, demonstrates the comparison of the measured $\alpha$-axis current command $i_\alpha$ and the measured $\beta$-axis current command $i_\beta$. The currents are the form of sinusoidal with amplitudes 0 *A*. There is some noise in this waveform to make the bandwidth of the current waveform.
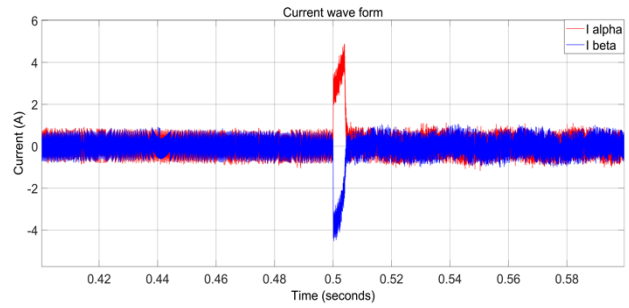


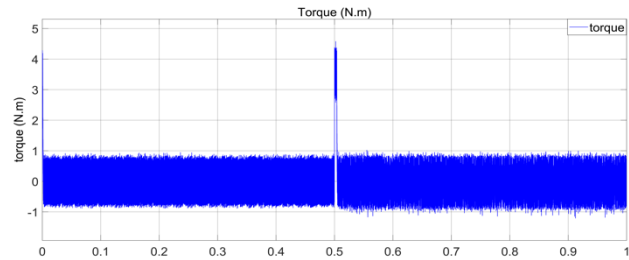**Fig. 7.** The current waveform of PMSM with no-load



**Fig. 8.** The load torque of PMSM

In this condition, the load torque of the PMSM is set to zero which means that the motor is spinning without load. Fig. 8, shows the graph of load torque at 0 *N.m* constantly with corrupted noise.
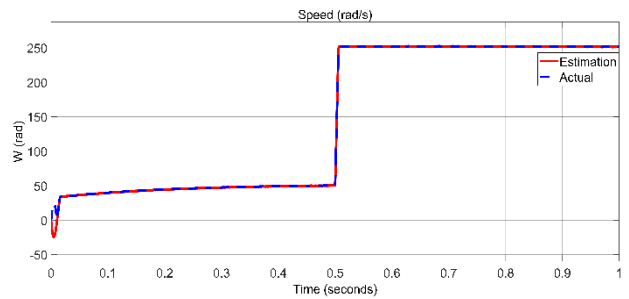


**Fig. 9.** Actual and estimated speed of PMSM with load

In case 2, Fig. 9 shows the comparison of rotor speed waveforms corresponding to the SMO methods. It can be seen that the estimated rotor speed is consistent with the actual rotor speed that the given target speed of the motor is 50 *rad/s* and changed to 250 *rad/s* at 0.5 *second* with constant load torque 4 *N.m* (maximum torque) is studied. The speed of PMSM with the load torque of 4 *N.m*. It can be seen that the speed response when start-up motor needs 0.4 *seconds* to reach the desired speed at 50 *rad/s*. The estimated speed is almost equal to the actual speed when it is stable, but there will be large chattering in the speed estimation at the moment of low speed and speed change. The SMO Observer can track reference speed accurately.

Fig. 10, shows the rotor position of PMSM while running at varying speeds and load torque. As shown in Fig. 10, the estimated value and actual value are started from different points. The estimated value started from 6 *rad* and the actual started from

0 *rad* then the estimate and actual were almost the same after the motor ran in a steady state. Due to the high-frequency chattering component, the estimated position of the rotor lags behind the actual position, and there is a fixed error, which cannot be corrected and improved and will affect the dynamic response performance of the system. The rotor position will change the wavelength when the speed of PMSM is varied too.
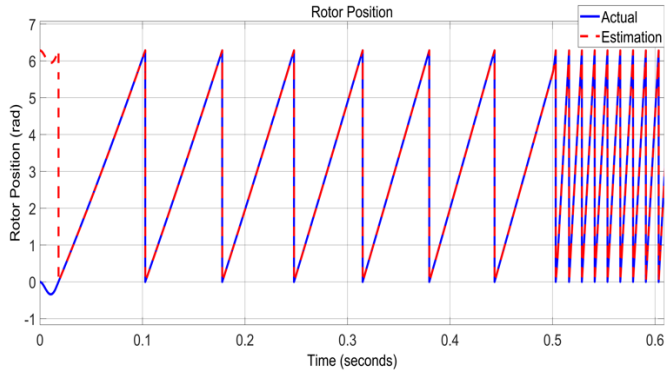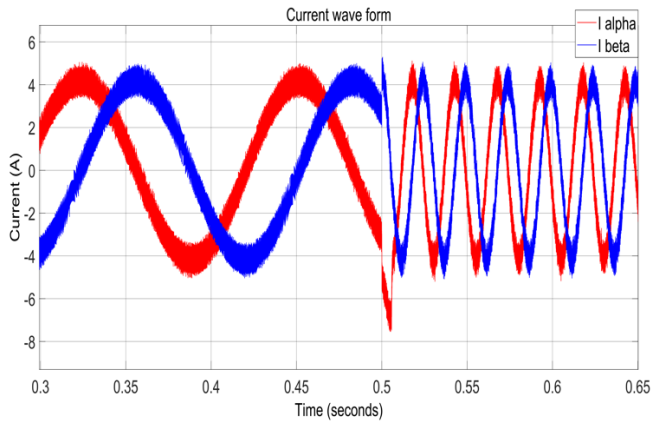


**Fig. 10.** Actual and estimated position of PMSM with load



**Fig. 11.** The current waveform of PMSM with load

Fig. 11 shows the current waveform of PMSM in $\alpha\beta$ frames. The currents are the form of sinusoidal with amplitude 4 *A*. There is some noise in this waveform and it will change the wavelength when the speed of PMSM is varied. The varies load torque, the currents also change the amplitudes. So when increasing load torque, the amplitude also increases, and when decreasing load torque, the amplitude also decreases as well.

Fig. 12, shows the output of the load torque of PMSM. This is the load torque applied in the system control of PMSM. The 4 *N.m* is the maximum load torque of the motor that is used constantly in the whole simulation.
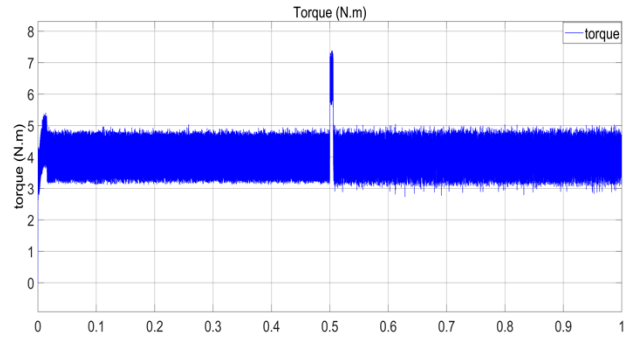


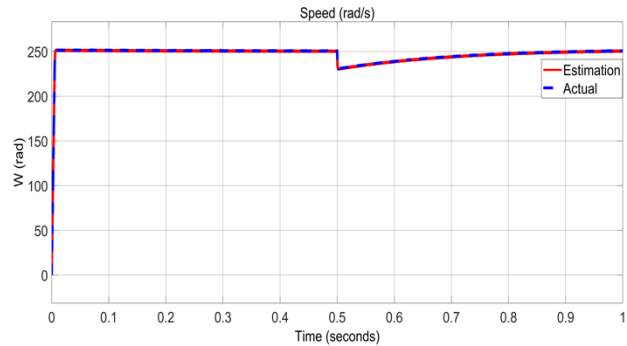**Fig. 12.** The varies load torque of PMSM



**Fig. 13.** Actual and estimate the constant speed of PMSM with varies load

In case 3, the performance of the sensorless system with constant speed at 270 *rad/s* and varying load torque from 0 *N.m* to 4 *N.m* at 0.5 *seconds* are tested. The simulation results are shown in Fig. 13, the speed of PMSM with varying load torque. It can be seen that the speed response when varied the load torque at 0.5 *second*, the motor needs 0.4 *second* to reach the desired speed at 270 *rad/s*. The SMO Observer can track the reference speed accurately. The corresponding speed waveform curve is much smoother. The estimated speed can quickly follow the set speed and converge to the actual speed, which shows that the system has good dynamic and static performance.
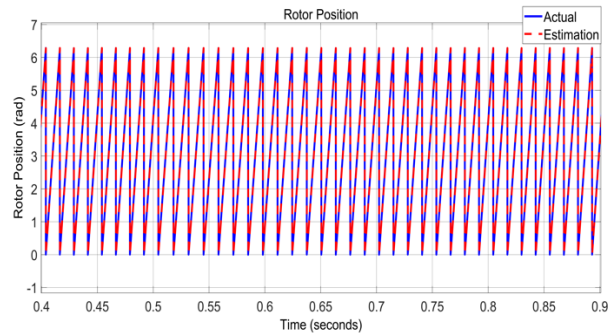


**Fig. 14.** Actual and estimated position with load

Fig. 14 shows the rotor position of PMSM with varying load torque. Therefore, the proposed sliding mode sensorless control

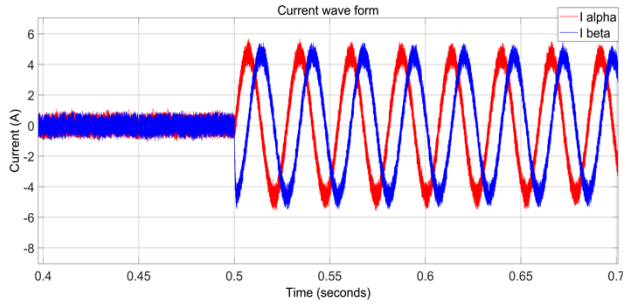algorithm can effectively estimate the speed and rotor position of the permanent magnet synchronous motor.



**Fig. 15.** The current waveform of PMSM with load

Fig. 15 shows the output step load torque of PMSM. In this condition, the load torque changes from 0 *N.m* (minimum load torque) to 4 *N.m* (maximum load torque) at 0.5 *seconds* for the simulation test. So when increasing load torque, the amplitude also increases as well.
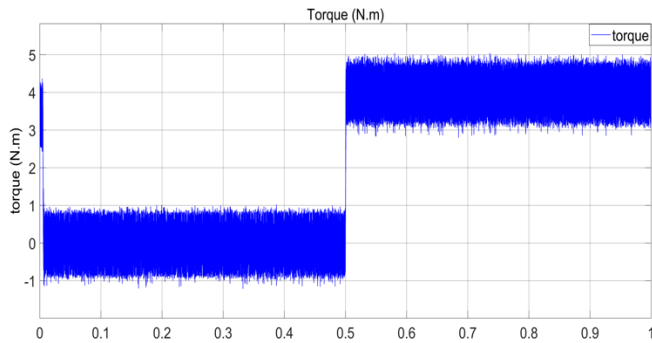


**Fig. 16.** The waveform varies load of PMSM

Fig. 16, shows the output step load torque of PMSM. In this condition, the load torque changes from 0 *N.m* (minimum load torque) to 4 *N.m* (maximum load torque) at 0.5 *seconds* for the simulation test.
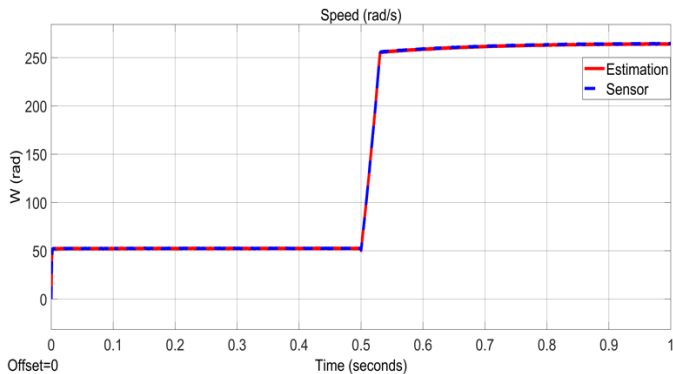


**Fig. 17.** Sensor and estimated speed of PMSM with sensors

In case 4, the simulation results of the sensors and estimated speed of the PMSM using sensors control with variable speeds

and torques are shown in Fig. 17. The performance of the sensors control with varying speeds from 50 *rad/s* to 260 *rad/s* at 0.5 *seconds* and varying load torque from 0 *N.m* (minimum load torque) to 3 *N.m* is studied. In Fig. 17, it can be seen that the speed response of the motor when no load torque is applied to the system, the motor reaches desired speed immediately (desire speed 50 *rad/s*) and started from 0.5 *seconds*, the load torque 3 *N.m* is applied. The motor needed 0.3 seconds to reach the desired speed of 260 *rad/s* at 0.8 *seconds* after applied load torque. For the sensors control with FOC when applied load torque, the feedback from sensors with the FOC method is not working well due to the PI controller but the SMO observer can be tracking accurately with speed measured by sensors although there is some oscillation when applying load torque and need time reach the desired speed.
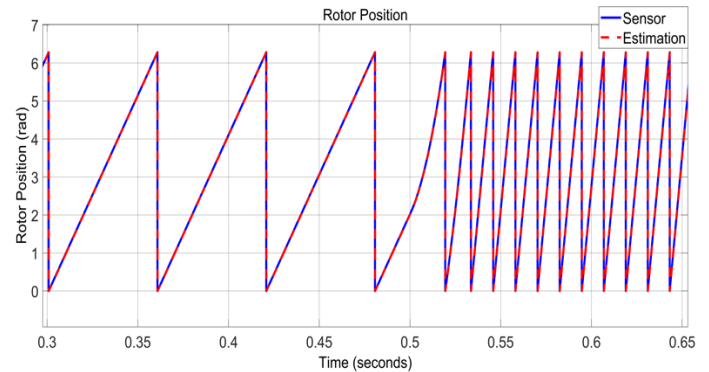


**Fig. 18.** Sensor and estimated rotor position of PMSM

Fig. 18 shows the rotor position of PMSM while running at various speeds and load torque with sensors. As the speed waveform, the rotor position also oscillates after applying the load torque but the SMO observer can well track the actual position of PMSM whatever the rotor position is changed at 0.5 *second*.
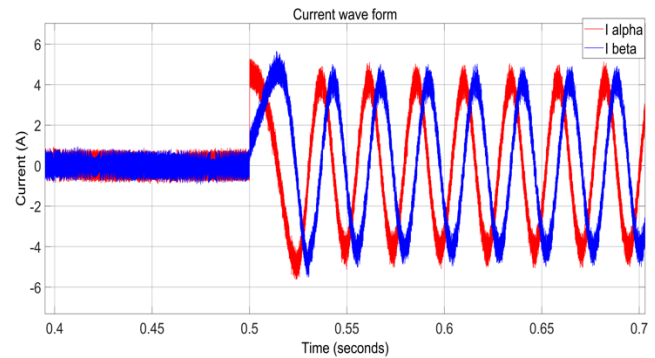


**Fig. 19.** The current waveform of PMSM with sensors

Fig. 19 shows the current waveform of PMSM in $\alpha\beta$ frames. The currents are the form sinusoidal with amplitude 0 *A* when no load torque and when 3 *N.m* of load torque is applied; the amplitude is changed too.
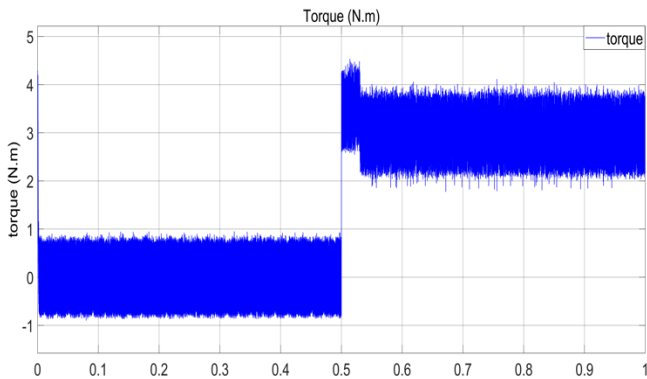
**Fig. 20.** The load torque of PMSM with sensors

Fig. 20 shows step load torque applied to the PMSM. In this condition, the load torque change from 0 *N.m* (minimum load torque) to 3 *N.m* at 0.5 *second* for the simulation test.

## 5. CONCLUSIONS

In this paper, the sensorless sliding mode observer for the permanent magnet synchronous motor is proposed for solar E-tuktuk application. Firstly, the sliding mode observer is studied and designed for sensorless control PMSM motors. From the sliding mode observer, we estimate the speed and rotor position and reduce the chattering by replacing the sign function with the continuous sigmoid function. The vector control operation of the drive is successfully demonstrated using MATLAB/Simulink base simulated results and discussed in section 4. The sensorless sliding mode control algorithm of permanent magnet synchronous motor is suitable for solar E-tuktuk by the system control has a fast response and robustness. The prototype setup will be implemented and tested in future work.

## ACKNOWLEDGMENTS

## REFERENCES

[1]   Semenov, D., Tian, B., An, Q. T., & Sun, L. (2016). Position estimation for sensorless FOC of five-phase PMSM in electric vehicles. *Proceedings of the 2016 Australasian Universities Power Engineering Conference, AUPEC 2016*. https://doi.org/10.1109/A UPEC.2016.07749286

[2]   El-samahy, A. A., & Shamseldin, M. A. (2018). Brushless DC motor tracking control using self-tuning fuzzy PID control and model reference adaptive control. *Ain Shams Engineering Journal*, *9*(3), 341–352. https://doi.org/10.1016/j.asej.2016.02.004

[3]   Kim, W. J., & Kim, S. H. (2018). A Sensorless V/f Control Technique based on MTPA Operation for PMSMs. *2018 IEEE Energy Conversion Congress and Exposition, ECCE 2018*, *4*, 1716–1721. https://doi.org/10.1109/ECCE.2018.8557412

[4]   Sharma, T., & Bhattacharva, A. (2019). Sensorless Direct Torque Control of PMSM Drive for EV Application. *2nd International Conference on Energy, Power and Environment: Towards Smart Technology, ICEPE 2018*. https://doi.org/10.1109/EPETSG.2018.8659157

[5]   Chaoui, H., & Sicard, P. (2015). *Almost Parameter-free Sensorless Control of*. 4667–4671.

[6]   Lehmann, O., Nguyen, N. K., Schuster, J., & Roth-Stielow, J. (2015). Optimized sensorless DTC of PMSM for electric vehicles by using a switching command synchronized evaluation at standstill and low speed. *9th International Conference on Power Electronics - ECCE Asia: "Green World with Power Electronics", ICPE 2015-ECCE Asia*, 1386–1393. https://doi.org/10.11 09/ICPE. 2015.7167960

[7]   Sreejith, R., & Singh, B. (2019). Intelligent Nonlinear Sensorless Predictive Field Oriented Control of PMSM Drive for Three Wheeler Hybrid Solar PV-Battery Electric Vehicle. *ITEC 2019 - 2019 IEEE Transportation Electrification Conference and Expo*. https://doi.org/10.1109/ITEC.2019.8790458

[8]   Haq, H., Hasan Imran, M., Okumus, H. I., & Habibullah, M. (2015). Speed Control of Induction Motor using FOC Method. *Journal of Engineering Research and Applications Www.Ijera.Com*, *5*(3), 154–158. www.ijera.com

[9]   Hezzi, A., Bensalem, Y., Ben Elghali, S., & Abdelkrim, M. N. (2019). Sliding Mode Observer based sensorless control of five phase PMSM in electric vehicle. *19th International Conference on Sciences and Techniques of Automatic Control and Computer Engineering, STA 2019*, *1*, 530–535. https://doi.org/10.1109/STA.2019. 8717290

[10]   Urbanski, K. (2015). Estimation of back EMF for PMSM at low speed range. *MM Science Journal*, *MAR 2015*, 564–569. https://doi.org/10.17973/mmsj.2015_03_201506

[11]   Li, Y., Wu, H., Xu, X., Sun, X., & Zhao, J. (2021). Rotor position estimation approaches for sensorless control of permanent magnet traction motor in electric vehicles: A review. *World Electric Vehicle Journal*, *12*(1), 1–26. https://doi.org/10.3390/WEVJ12010009

[12]   Tian, G., Yan, Y., Jun, W., Ru, Z. Y., & Peng, Z. X. (2018). Rotor Position Estimation of Sensorless PMSM Based on Extented Kalman Filter. *2018 IEEE International Conference on Mechatronics, Robotics and Automation, ICMRA 2018*, 12–16.

[13]   Tang, H., Li, H., & Lin, J. (2018). Research on sensorless control method of PMSM based on a kalman filter sliding mode observer. *Proceedings - 10th International Conference on Measuring Technology and Mechatronics*

*Automation, ICMTMA 2018, 2018-Janua*(8), 290–293. https://doi.org/10.1109/ICMTMA.2018.00077

[14] Urbanski, K., & Janiszewski, D. (2019). Sensorless control of the permanent magnet synchronous motor. *Sensors (Switzerland)*, *19*(16). https://doi.org/10.3390/ s19163546

[15] Zhang, X., Tian, G., Huang, Y., & Lu, Z. (2016). A Comparative Study of PMSM Sensorless Control Algorithms: Model Based vs Luenberger Observer. *2016 IEEE Vehicle Power and Propulsion Conference, VPPC 2016 - Proceedings*. https://doi.org/10.1109/VPPC.20 16.7791566

[16] MMahawar, J. K., & Dahiya, A. K. (2020). Parmanent Magnet Synchronous Motor Control Based on Model Reference Adaptive Approach. *2020 11th International Conference on Computing, Communication and Networking Technologies, ICCCNT 2020*, 5. https://doi.org/10.1109/ICCCNT49239.2020.9225545

[17] Yousfi, D., Elbacha, A., & Ait, A. (2011). Efficient Sensorless PMSM Drive for Electric Vehicle Traction Systems. *Electric Vehicles - Modelling and Simulations*. https://doi.org/10.5772/16600

[18] Bedetti, N., Calligaro, S., & Petrella, R. (2013). A novel approach to the design of back-EMF observer based sensorless control of non-salient PMSM: Theoretical analysis and experimental investigations. *2013 IEEE Energy Conversion Congress and Exposition, ECCE 2013*, *September*, 3496–3503.

[19] Lee, J. W. (2015). Adaptive sensorless control of high speed PMSM with back EMF constant variation. *9th International Conference on Power Electronics - ECCE Asia: "Green World with Power Electronics", ICPE 2015-ECCE Asia*, *1*, 1400–1404. https://doi.org/10.1109 /ICPE.2015.7167962

[20] Zhang, T., Xu, Z., Li, J., & Yan, H. (2019). Enhanced Speed Extraction for Salient PMSM Sensorless Drives Based on A Cascaded Extended State Observer. *2018 IEEE International Conference on Electrical Systems for Aircraft, Railway, Ship Propulsion and Road Vehicles and International Transportation Electrification Conference, ESARS-ITEC 2018*, 1–6. https://doi.org/10.1109/ESARS-ITEC.2018.8607733

[21] Xu, Y. T., Wang, Z. H., & Zhao, H. L. (2016). Position sensorless control of PMSM based on Extended State Observer. *2015 12th International Computer Conference on Wavelet Active Media Technology and Information Processing, ICCWAMTIP 2015*, 369–373.

[22] Sreejith, R., & Singh, B. (2018). Improved Sliding Mode Observer based Position Sensorless Finite Control Set-Model Predictive Control of PMSM Drive for Electric Vehicle. *India International Conference on Power Electronics, IICPE, 2018-Decem*, 1–6. https://doi.org/10.1109/IICPE.2018.8709544

[23] Sun, L., Zhang, X., Sun, L., & Zhao, K. (2013). Nonlinear speed control for PMSM system using sliding-mode control and disturbance compensation techniques. *IEEE Transactions on Power Electronics*, *28*(3), 1358–1365. https://doi.org/10.1109/TPEL.2012.2206610

[24] Kim, H., Son, J., & Lee, J. (2011). A high-speed sliding-mode observer for the sensorless speed control of a PMSM. *IEEE Transactions on Industrial Electronics*, *58*(9), 4069–4077. https://doi.org/10.1109/TIE.20 10.2098357

[25] Rong, Y., Jiao, R., Kang, S., & Chou, W. (2019). Sigmoid super-twisting extended state observer and sliding mode controller for quadrotor UAV attitude system with unknown disturbance. *IEEE International Conference on Robotics and Biomimetics, ROBIO 2019*, *December*, 2647–2653.
https://doi.org/10.1109/ROBIO49542.2019.8961654

[26] Liang, Y. W., Xu, S. D., Cheng, C. C., & Liaw, D. C. (2008). Design of robustly asymptotic stabilizer using a time-varying sigmoid-type SMC scheme. *Proceedings of the IEEE International Conference on Industrial Technology*, 2–6. https://doi.org/10.1109/ICIT.200 8.4608411

[27] Sreejith, R., & Singh, B. (2021). Sensorless Predictive Current Control of PMSM EV Drive Using DSOGI-FLL Based Sliding Mode Observer. *IEEE Transactions on Industrial Electronics*, *68*(7), 5537–5547. https://doi.org/10.1109/TIE.2020.2996159